

## Recent results from Fermi-LAT

F. DE PALMA on behalf of the FERMI LAT COLLABORATION

*INFN, Sezione di Bari - Bari, Italy*

ricevuto il 7 Settembre 2012

**Summary.** — We highlight the most important recent results from the Fermi Large Area Telescope (LAT). The latest source catalog (2FGL) is briefly discussed and several recent results on DM indirect searches from different targets are summarized. Finally, various results on the cosmic rays direct detection are presented.

PACS 95.85.Pw –  $\gamma$ -ray.

PACS 95.80.+p – Astronomical catalogs, atlases, sky surveys, databases, retrieval systems, archives, etc.

PACS 95.35.+d – Dark matter (stellar, interstellar, galactic, and cosmological).

PACS 96.50.S- – Cosmic rays.

### 1. – The LAT instrument

The LAT is a pair conversion detector on board the Fermi Gamma-ray Space Telescope. It began its nominal science operations on August 4, 2008. It is designed to measure the directions, energies, and arrival times of  $\gamma$ -rays incident over a wide Field of View (FoV  $\sim 2.4$ sr), while rejecting background from charged cosmic rays. To take full advantage of the LAT large FoV, the primary observing mode of Fermi is the so-called scanning mode that ensures an almost uniform sky coverage every two orbits ( $\sim 3$  hours). In case of particularly interesting targets of opportunity, the observatory can be inertially pointed either by issuing a command from the ground, or autonomously in the occurrence of a Gamma-ray Burst (GRB).

The LAT is composed by a precision converter-tracker and a calorimeter, each consisting of a  $4 \times 4$  array of towers. A segmented anti coincidence detector (ACD), for the rejection of the charged-particle background, covers the tracker array [1-3]. Different event selections were developed for the various analysis that can be done with the LAT data and three different cuts were applied to select public data samples with increasing levels of purity, see [3] and the LAT performance web page<sup>(1)</sup>.

<sup>(1)</sup> [http://www.slac.stanford.edu/exp/glast/groups/canda/archive/pass7v6/lat\\_Performance.htm](http://www.slac.stanford.edu/exp/glast/groups/canda/archive/pass7v6/lat_Performance.htm)

## 2. – The 2FGL source catalog

The second Fermi LAT source catalog (2FGL) [4] represents the most complete catalog of  $\gamma$ -ray sources in the 100 MeV–100 GeV energy range. Source detection is based on the average flux over the 24 month period. The 2FGL includes source locations and spectral fits in terms of power-law, power-law with exponential cutoff, or log-normal forms. Also included are flux measurements and statistical significance in five energy bands, light curves on monthly intervals for each source and a variability index. Twelve sources in the catalog are modeled as spatially extended with different shapes and sizes. The analysis was performed applying the new event P7SOURCE\_V6 [3] selections and using a new and highly-resolved model of the diffuse Galactic and isotropic emissions. All the results are summarized in FITS files<sup>(2)</sup> and are publicly available from the FSSC web page<sup>(3)</sup>. The sources reported in the 2FGL have a statistical significance of at least  $4\sigma$  above the background (see [4]).

As in the two previous LAT source catalogs [5,6], in the 2FGL the distinction between associations and firm identifications is kept. Although many associations, particularly those for AGNs, have very high probability of being true, a firm identification is based on one of the following three criteria:

1. Periodic Variability and Pulsations. Pulsars are the larger class in this category but binaries are also included.
2. Spatial Morphology. Spatially extended sources whose morphology can be related to the shape seen at other wavelengths include SNR, PWNe, and galaxies.
3. Correlated Variability. Variable sources, primarily AGNs, whose  $\gamma$ -ray variability can be matched to that seen at one or more other wavelengths, are considered to be firm identifications.

In total, we firmly identify 127 out of the 1873 2FGL sources. The algorithm for the associations is described in [4] and in [6]. In summary, we use a Bayesian approach that trades the positional coincidence of possible counterparts with 2FGL sources against the expected number of chance coincidences to estimate the probability that a specific counterpart association (in other catalogs) is indeed real (*i.e.*, a physical association). We retain counterparts as associations if they reach a posterior probability of at least 80%.

Among the 1873 sources in the 2FGL catalog, 575 (31%) remain unassociated. This could be due to both a incomplete catalog coverage at  $|b| < 10^\circ$  and to some systematic uncertainties in the galactic model. 162 sources are flagged to indicate possible confusion with residual imperfections in the diffuse model.

The next years will allow to detect and observe even fainter sources and increase the statistics for population studies, allowing us to better constrain different emission models of the various sources. Above 10 GeV, Fermi is starting to detect large-scale regions of excess high-energy emission not predicted by interstellar emission models, including the “*Fermi lobes*” [7] and other large-scale hard-spectrum diffuse features. At these energies more than 500 sources have been detected, and around 170 of these sources are still unassociated and are not observed at other energies. Since the photon statistics are still

---

<sup>(2)</sup> <http://fits.gsfc.nasa.gov/>

<sup>(3)</sup> [http://fermi.gsfc.nasa.gov/ssc/data/access/lat/2yr\\_catalog/](http://fermi.gsfc.nasa.gov/ssc/data/access/lat/2yr_catalog/)

low in this energy range, we will likely continue to find new sources during the next years of observations.

Using a 36 months data sample 101 pulsars have been found and 16 SNRs have been studied. With the forthcoming SNR LAT catalog more sources could be found and studied and a better understanding of the emission region and mechanism will follow. The study and identification of nearby sources of photons and possibly of cosmic rays is of fundamental importance also for other analysis of the LAT data that will be described in the following sections.

### 3. – Dark Matter search strategy

In the following subsections some of the main targets for the indirect Dark Matter (DM) signal search with the Fermi data will be shown.

**3.1. Dwarfs satellites.** – Milky Way dwarf spheroidal (dSph) galaxies are good candidate targets for DM studies through annihilation signatures, because their mass-to-light ratio is predicted to be of the order of  $10\text{--}10^3$  [8], implying that they could be largely DM dominated. Moreover, since no significant  $\gamma$ -ray emission of astrophysical origin is expected (these systems host few stars and no hot gas), the detection of a  $\gamma$ -ray signal could provide a clean DM signature. Weakly Interacting Massive Particles (WIMPs) have long been considered as well-motivated candidates for DM that could contribute to the 80% of the non-baryonic mass density in the universe. At a given energy  $E$ , the differential  $\gamma$ -ray flux  $\Phi_\gamma(E, \Delta\Omega)$  from WIMP annihilation in a region covering a solid angle  $\Delta\Omega$  and centered on a DM source, can be factorized as [9]

$$(1) \quad \Phi_\gamma(E, \Delta\Omega) = J(\Delta\Omega) \times \Phi^{PP}(E),$$

where  $J(\Delta\Omega)$  is the “*astrophysical factor*” or  $J$ -factor, *i.e.* the line of sight (l.o.s.) integral of the DM density squared in the direction of observation over the solid angle  $\Delta\Omega$ . The term  $\Phi^{PP}(E)$  is the “*particle physics factor*”, that encodes the particle physics properties of the DM as the mass of the WIMP ( $m_\chi$ ) and various parameters that describe the annihilation.  $\Phi^{PP}(E)$  depends linearly to  $\langle\sigma v\rangle$ , *i.e.* the WIMP pair annihilation cross-section times the relative velocity of the two annihilating particles.

Even if the  $J$ -factor is different for each dSph, the characteristics of the WIMP candidate ( $m_W$ ,  $\langle\sigma_{\text{ann}}v\rangle$ , annihilation channels and their branching ratios) can be assumed to be universal and so different sources can be studied together.

In [10] 24 months of P6V3 *diffuse* class events [3] between 200 MeV and 100 GeV are analyzed. Using the newly developed *composite2* likelihood technique, the DM signals across 10 Regions of Interest (ROIs), each associated to a different dSph, are combined while the other diffuse models and point sources are fitted separately. Uncertainties on the  $J$ -factor are taken into account in the fit procedure by adding a proper term to the likelihood that represents the measurement uncertainties. As no significant signal is found, upper limits were reported (see fig. 1). These upper limits allow us to rule out WIMP annihilation with cross-sections predicted by the most generic cosmological calculations up to a mass of  $\sim 27$  GeV for the  $b\bar{b}$  channel and up to a mass of  $\sim 37$  GeV for the  $\tau^+\tau^-$  channel. More stringent upper limits could be obtained in the future with more data (in 10 years an improvement of a factor of 5) and with new dSphs. In [11] these limits are compared with the predictions of a large number of different models.

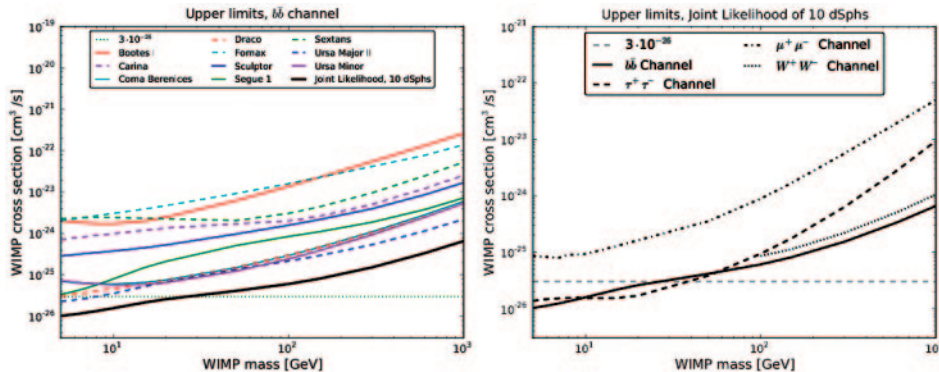


Fig. 1. – Left panel: derived 95% CL upper limits on a WIMP annihilation cross-section for all selected dSphs and for the joint likelihood analysis for annihilation into the  $b\bar{b}$  final state. Right panel: derived 95% CL upper limits on the WIMP annihilation cross-section for all the four channels studied in [10]  $b\bar{b}$ ,  $\tau^+\tau^-$ ,  $\mu^+\mu^-$  and  $W^+W^-$ . The most generic cross-section ( $\sim 3 \cdot 10^{-26} \text{ cm}^3 \text{ s}^{-1}$  for a purely  $s$ -wave cross-section) is shown as a reference in both plots. Uncertainties in the  $J$ -factor are included in all the analyses. Taken from [10].

Another approach to this analysis is described in [9]. In this case the same set of dSphs were used, but the analysis was performed with 3 years of P7SOURCE.V6 data [3] in the energy range from 562 MeV to 562 GeV implementing a model independent approach. A signal region of  $0.5^\circ$  and a background region consisting of an annulus between  $5^\circ$  and  $6^\circ$  around each dSph were selected. The upper limits were evaluated with a Bayesian technique on each dSph and for all the ten sources with two different procedures, using the average  $J$ -factor or the proper  $J$ -factors of each source. The upper limits on the signal counts were finally converted into upper limits on the flux by means of an unfolding procedure (see [9] and references therein). These results, even though obtained with a different event reconstruction and a different technique are similar and consistent with the previous ones.

**3.2. Clusters.** – Clusters of galaxies are the most massive objects in the Universe that have had time to virialize by the present epoch, making nearby clusters attractive targets for searches for a signature from DM annihilation. Clusters are more distant, but also more massive than dSph galaxies, and like dSphs, they are very DM dominated, and typically lie at high galactic latitudes where the contamination from Galactic  $\gamma$ -ray background is low. Unlike in dSphs, DM annihilation is not the only potential source of  $\gamma$ -ray emission because several astrophysical mechanisms can occur. Significant  $\gamma$ -ray emission has not been detected from local clusters by the Fermi-LAT in the first 11 months of observation [12] and a recent preliminary analysis on 24 months of data for 6 clusters did not show any excess in the stacked residual maps. These results provided some tight limits on DM models, even though in literature there are different analysis that show the possibility of a faint signal (*e.g.*, [13]).

**3.3. Milky Way.** – The DM annihilation in the Milky Way halo is another target for DM search due to the large DM density expected in the vicinity of the Galactic Center and the proximity of the region. The analysis in this region is done with both the profile likelihood technique [14] and the Bayesian technique [10]. In the first approach, various

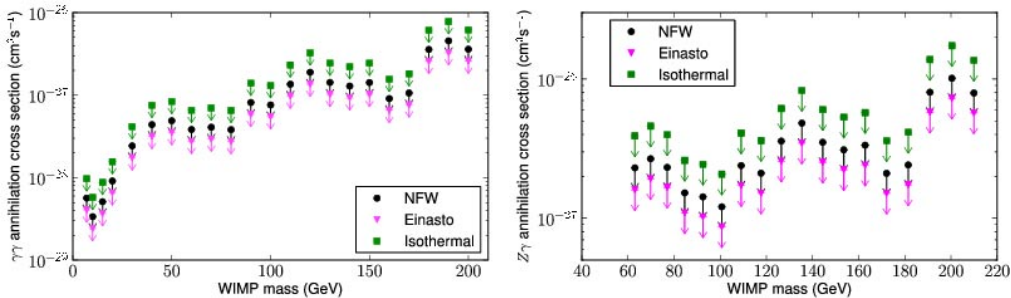


Fig. 2. – Dark matter annihilation 95% CL cross-section upper limits into  $\gamma\gamma$  (left) and  $Z\gamma$  (right) for the NFW, Einasto, and isothermal profiles for the region  $|b| > 10^\circ$  plus a  $20^\circ \times 20^\circ$  square centered on the Galactic center.  $\gamma Z$  limits below  $E_\gamma < 30$  GeV are not shown. Taken from [17].

limits are evaluated, from the most conservative one (assuming that all the detected photons from the halo are produced by annihilating/decaying WIMPs), to the deepest one (using GALPROP [15] simulations to model the astrophysical diffuse background). The limits derived for leptonic models challenge the interpretation of the PAMELA and Fermi cosmic rays anomalies (see sect. 4) as annihilation of DM in the Galactic Halo, while they are not enough constraining to exclude the interpretation in terms of decaying DM. In [10] just the most conservative approach is used, and 1000 random locations are selected to set upper limits that are consistent with the previous.

The Galactic center is also a good candidate to observe the DM annihilation signal due to the large quantity of DM that should be located in that region, even though it is one of the most crowded and complex region in the sky. A preliminary analysis with 3 years of P7 data [3] has shown that the galactic diffuse component and some point sources can account for the observed emission and no strong structures are found in residuals maps.

**3.4. Spectral lines from WIMPs.** – In [16] and [17] a search for monochromatic  $\gamma$ -rays from WIMPs annihilation or decay is performed. If a WIMP annihilates or decays directly into a photon ( $\gamma$ ) and another particle ( $X$ ), the photons are approximately monochromatic. Detection of one or more striking spectral lines would be convincing evidence for DM. Using a set of 2 years P6 DATACLEAN [3] data no evidence for photon lines was found. Starting from the evaluated upper limits at 95% CL on the spectral line and assuming three different spatial distribution of DM, it is possible to evaluate the upper limits on the annihilation cross-section on both the  $\gamma\gamma$  channel and the  $Z\gamma$  channel (see bottom panel of fig. 2 and for a complete discussion see [17]). Theoretical predictions for  $\gamma$ -ray line intensity are highly model dependent, so that only some models are constrained by this results. In literature (*e.g.*, [18]) some analyses that have found a hint of a possible detection can be found.

**3.5. Isotropic diffuse background.** – In [19] and [20] the full-sky  $\gamma$ -ray survey is performed for searching a possible isotropic DM signal, originating from annihilations summed over halos at all redshifts. Most cosmological halos are individually unresolved and will contribute to an approximately isotropic  $\gamma$ -ray background radiation (IGRB). The difficulty of estimating the isotropic background to the cosmological DM annihilation signal further increases the uncertainty in these limits. Blazars, radio galaxies

and star-forming galaxies account from 50% to 80% of the observed extragalactic background light spectra. Given these uncertainties, in [19] the most conservative and most optimistic limits on cross-sections span three orders of magnitude. While the most conservative constraints barely reach exclusion of theoretically discussed DM cross-sections, more optimistic descriptions of the DM halos and subhalos would instead allow to exclude several models.

#### 4. – The LAT as an electron detector

Since electromagnetic (EM) cascades are generated during both electron and photon interactions in matter, the LAT is also by its nature a detector for electrons and positrons. For event reconstruction (track identification, energy and direction measurement, ACD analysis) and calculation of variables used in event classification we use the same reconstruction algorithms as for photons. The selections are of course different and specific to the electron analysis. The high flux of cosmic-rays (CRs) protons and helium compared to that of electrons and positrons dictates that the hadron rejection must be  $10^3$ – $10^4$ , increasing with energy, which can be reached analysing the shape of the shower.

*4.1. Electron and positron combined spectra.* – The observed spectra in [21], from 7 GeV to 1 TeV can be fitted by a power law with spectral index in the interval 3.03–3.13 (best fit 3.08), similar to that given in [22]. The spectrum is significantly harder than that reported by previous experiments with the absence of any evident feature. In any case, some spectral flattening at 70–200 GeV and a noticeable excess above 200 GeV are suggested, as compared to the power-law spectral fit. The gentle features of the spectrum can be explained within a conventional model by adjusting the injection spectra. Another possibility that provides a good overall agreement with our spectrum is the introduction of an additional leptonic component with a hard spectrum. Such an additional component is motivated by the rise in the positron fraction reported by PAMELA [23] and the LAT (see sect. 4.2). Different kinds of models can explain this component, from nearby sources (such as pulsars) to the annihilation of DM particles (see [21] for more references).

*4.2. Electron and positron separate spectra.* – The LAT can also measure separately the spectra of CR electrons (CREs) and positrons from 20 GeV to 200 GeV, taking advantage of the Earth shadow and the offset direction for electrons and positrons due to the geomagnetic field, as fully described in [24]. This is the first time that the absolute CR positron spectrum has been measured above 50 GeV and that the fraction has been determined above 100 GeV, as shown in fig. 3. We find that the positron fraction increases with energy between 20 and 200 GeV, in agreement with the results reported by PAMELA [23]. The best established mechanism for producing CR positrons is secondary production. Such secondary production will result in a positron fraction that decreases with energy. The origin of the rising positron fraction at high energy is unknown and has been ascribed to a variety of mechanisms including additional contribution from pulsars and SNRs, CRs interacting with giant molecular clouds, and DM (see [24] and references therein). Future measurements with greater sensitivity and energy reach, such as those by AMS-02, are necessary to distinguish between the many possible explanations of this increase.

*4.3. Cosmic-ray electron anisotropy.* – In [25] the arrival directions of the reconstructed cosmic-ray electrons and positrons were searched for anisotropies at angular scales extending from  $\sim 10^\circ$  up to  $90^\circ$ . Any anisotropy in the arrival directions of



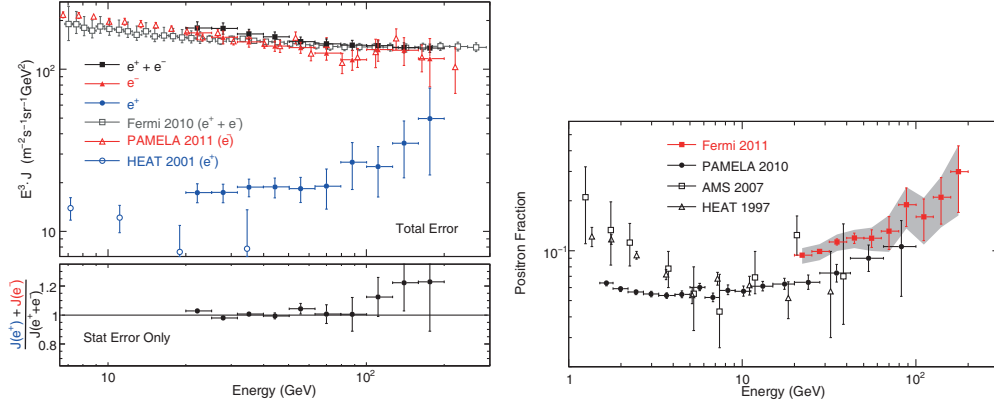


Fig. 3. – On the left: energy spectra for  $e^+$ ,  $e^-$ , and  $e^+ + e^-$  (control region). In the control region where both species are allowed, this analysis reproduces the Fermi LAT results reported previously for the total electron plus positron spectrum [22, 21] (gray). The bottom panel shows that the ratio between the sum and the control flux is consistent with 1 as expected. On the right: positron fraction measured by the Fermi LAT and by other experiments. The Fermi statistical uncertainty is shown with error bars and the total (statistical plus systematic uncertainty) is shown as a shaded band. For the full list of reference and for more details see [24].

cosmic-ray electrons (CREs) detected by the LAT would be a powerful tool to discriminate between a DM origin and an astrophysical one. In particular, since Galactic DM is denser towards the direction of the Galactic center, the generic expectation in the DM annihilation or decay scenario is a dipole with an excess towards the center of the Galaxy and a deficit towards the anti-center. Also, both the Monogem and the Geminga pulsars, likely some of the most significant CRE sources, are both roughly placed opposite to the direction of the Galactic Center, making a search for anisotropy an effective distinguishing diagnostic. Two independent techniques were applied, both resulting in null results. Upper limits on the degree of the anisotropy were set, for different energy ranges and angular scale. The upper limits for a dipole anisotropy ranged from  $\sim 0.5\%$  to  $\sim 10\%$ . These limits were compared with the predicted anisotropies from individual nearby pulsars and from DM annihilations, in all cases, they lie roughly above the predicted anisotropies.

**4.4. High-energy cosmic-ray electrons from the Sun.** – In [26] we use the high-energy cosmic-ray electron and positron (CRE) data set to search for flux variations correlated with the Sun direction. No known astrophysical mechanisms are expected to generate a significant high-energy CRE ( $> 100$  GeV) excess associated with the Sun, while several classes of DM models could generate this kind of emission.

In some scenarios DM particles captured by the Sun through elastic scattering interactions would annihilate to  $\phi$  (a new light intermediate state) pairs in the Sun's core, and if the  $\phi$  could escape the surface of the Sun before decaying to CREs, these can be detected by the LAT. In other scenarios DM is captured by the Sun only through inelastic scattering (iDM), this could lead to a non-negligible fraction of DM annihilating outside the Sun's surface. For models in which iDM annihilates to CREs, an observable flux at energies above a few tens of GeV could be produced.

In the case of annihilation of DM through an intermediate state and subsequent decay to  $e^\pm$ , the upper limits on solar CRE fluxes provide significantly stronger constraints on the DM scattering cross-section than limits previously derived by constraining the final state radiation emission associated with this decay channel using solar  $\gamma$ -ray measurements. For the iDM scenario, the solar CRE flux upper limits exclude the range of models which can reconcile the data from DAMA/LIBRA and CDMS for  $m_\chi \gtrsim 70$  GeV, assuming DM annihilates predominantly to  $e^\pm$ . Since direct detection experiments are not sensitive to the dominant annihilation channels of the DM particles, other data, *e.g.*, solar  $\gamma$ -ray measurements and neutrino searches, may be able to further constrain these models by excluding regions of parameter space for alternative annihilation channels.

\* \* \*

The *Fermi* LAT Collaboration acknowledges support from a number of agencies and institutes for both development and the operation of the LAT as well as scientific data analysis. These include NASA and DOE in the United States, CEA/Irfu and IN2P3/CNRS in France, ASI and INFN in Italy, MEXT, KEK, and JAXA in Japan, and the K. A. Wallenberg Foundation, the Swedish Research Council and the National Space Board in Sweden. Additional support from INAF in Italy and CNES in France for science analysis during the operations phase is also gratefully acknowledged.

## REFERENCES

- [1] ATWOOD W. B. *et al.*, *Astrophys. J.*, **697** (2009) 1071.
- [2] ABDO A. A. *et al.*, *Astropart. Phys.*, **32** (2009) 193.
- [3] FERMI-LAT COLLABORATION, *Astrophys. J. Suppl. S.*, **203** (2012) 4.
- [4] NOLAN P. L. *et al.*, *Astrophys. J. Suppl. S.*, **199** (2012) 31.
- [5] ABDO A. A. *et al.*, *Astrophys. J. Suppl. S.*, **183** (2009) 46.
- [6] ABDO A. A. *et al.*, *Astrophys. J. Suppl. S.*, **188** (2010) 405.
- [7] SU M., SLATYER T. R. and FINKBEINER D. P., *Astrophys. J.*, **724** (2010) 1044.
- [8] STRIGARI L. E. *et al.*, *Nature*, **454** (2008) 1096.
- [9] MAZZIOTTA M. N. *et al.*, *Astropart. Phys.*, **37** (2012) 26.
- [10] ACKERMANN M. *et al.*, *Phys. Rev. Lett.*, **107** (2011) 241302.
- [11] COTTA R. C. *et al.*, *J. Cosm. Astropart. Phys.*, **4** (2012) 16.
- [12] ACKERMANN M. *et al.*, *J. Cosm. Astropart. Phys.*, **5** (2010) 25.
- [13] HAN J. *et al.*, arXiv:1201.1003 (2012).
- [14] ACKERMANN M. *et al.*, arXiv:1205.6474 (2012).
- [15] STRONG A. W., MOSKALENKO I. V. and REIMER O., *Astrophys. J.*, **537** (2000) 763.
- [16] ABDO A. A. *et al.*, *Phys. Rev. Lett.*, **104** (2010) 091302.
- [17] ACKERMANN M. *et al.*, *Phys. Rev. D*, **86** (2012) 022002.
- [18] WENIGER C., arXiv:1204.2797 (2012).
- [19] ABDO A. A. *et al.*, *J. Cosm. Astropart. Phys.*, **4** (2010) 14.
- [20] ACKERMANN M., *Talk at the TeVPA 2011 conference, 1-5 Aug. 2011, Stockholm, Sweden.*
- [21] ACKERMANN M. *et al.*, *Phys. Rev. D*, **82** (2010) 092004.
- [22] ABDO A. A. *et al.*, *Phys. Rev. Lett.*, **102** (2009) 181101.
- [23] ADRIANI O. *et al.*, *Nature*, **458** (2009) 607.
- [24] ACKERMANN M. *et al.*, *Phys. Rev. Lett.*, **108** (2012) 011103.
- [25] ACKERMANN M. *et al.*, *Phys. Rev. D*, **82** (2010) 092003.
- [26] AJELLO M. *et al.*, *Phys. Rev. D*, **84** (2011) 032007.